OPEN

Original article

Nuclear Medicine Communications

Precise quantitative evaluation of pharmacokinetics of cisplatin using a radio-platinum tracer in tumor-bearing mice

Honoka Obata[a,b,c], Atsushi B. Tsuji[b], Hitomi Sudo[b], Aya Sugyo[b], Katsuyuki Minegishi[a], Kotaro Nagatsu[a], Mikako Ogawa[c] and Ming-Rong Zhang[a]

Objective **The platinum-based antineoplastic drug cisplatin is commonly used for chemotherapy in clinics. This work aims to demonstrate a radio-platinum tracer is useful for precisely quantifying small amounts of platinum in pharmacokinetics studies.**

Methods **A cisplatin radiotracer (radio-cisplatin) was synthesized, and a comprehensive evaluation of cisplatin over 7 days after its intravenous injection into nude mice bearing a subcutaneous lung tumor (H460) was conducted.**

Results **A biphasic retention curve in the whole body and blood was observed [$T_{1/2}(\alpha) = 1.14$ h, $T_{1/2}(\beta) = 5.33$ days for the whole body, and $T_{1/2}(\alpha) = 23.9$ min, $T_{1/2}(\beta) = 4.72$ days for blood]. The blood concentration decreased within 1 day after injection. Most of the intact cisplatin was excreted via the kidneys in the early time points, and a small part was distributed in tissues including tumors. The plasma protein binding rate of cisplatin increased rapidly after injection, and the protein-bound cisplatin remained in the blood longer than intact cisplatin. The peak uptake in H460 tumors was 4.7% injected dose per gram at 15 min after injection, and the area under the curve ($AUC_{0-7\ days}$) was approximately one-half to one-third of the $AUC_{0-7\ days}$ in the kidneys, liver, and bone, where some toxicity is observed in humans.**

Conclusion **The radio-platinum tracer revealed the highly quantitative biodistribution of cisplatin, providing insights into the properties of cisplatin, including its adverse effects. The tracer enables a precise evaluation of pharmacokinetics for platinum-based drugs with high sensitivity. *Nucl Med Commun* 43: 1121–1127 Copyright © 2022 The Author(s). Published by Wolters Kluwer Health, Inc.**

Nuclear Medicine Communications 2022, **43**:1121–1127

Keywords: biodistribution, cisplatin, lung cancer, pharmacokinetics, radio-platinum

Departments of [a]Advanced Nuclear Medicine Sciences and [b]Molecular Imaging and Theranostics, National Institutes for Quantum Science and Technology (QST), Chiba and [c]Graduate School of Pharmaceutical Sciences, Hokkaido University, Sapporo, Japan

Correspondence to Atsushi B. Tsuji, PhD, Department of Molecular Imaging and Theranostics, National Institutes for Quantum Science and Technology (QST), 4-9-1 Anagawa, Inage-ku, Chiba 263-8555, Japan
Tel: +81 43 382 3704; e-mail: tsuji.atsushi@qst.go.jp

Received 1 June 2022 **Accepted** 23 August 2022

Introduction

Platinum (Pt) is a promising metal element in pharmaceuticals for cancer therapy, and numerous Pt-based antineoplastic drugs have been developed [1]. *cis*-diamminedichloroplatinum (*cis*-[$Pt^{II}Cl_2(NH_3)_2$]), commonly called cisplatin, is a widely used chemotherapeutic agent, and its value is supported by a large number of basic and clinical studies [2]. The generic drug cisplatin has been applied to almost all tumor types because it acts by simply forming various direct DNA–Pt adducts such as intra- and interstrand cross-links, leading to cell death [3–6]. However, it cannot specifically target tumor cells, causing adverse renal effects [7]. To decrease such unwanted side effects, next-generation tumor-targeting Pt drugs have been attracting interest in the chemotherapeutics field in recent years [1]. A method that enables the precise and practical quantitation of Pt has the potential to promote studies of the pharmacokinetics of Pt drugs.

Numerous studies have evaluated the pharmacokinetics of Pt drugs using HPLC, atomic absorption analysis, or inductively coupled plasma–mass spectrometry [8–12]. Although these chemical analysis methods are common, they require at least nanogram quantities of Pt for precise quantification. Fluorescent imaging offers high sensitivity but is unsuitable for tracing Pt ideally because labeling Pt drugs with a fluorescent dye likely changes their behavior. Because of this experimental limitation in precisely quantifying small amounts of Pt, previous studies have mainly focused on blood or urine retention in the case of high injection doses for humans [9–12]; biodistribution data are rare, especially in the case of a low injection dose, long-term tracing, or low-uptake tissue retention. Efficient methods and detailed results of the biodistribution of Pt will contribute to the further development of Pt-based drugs.

0143-3636 Copyright © 2022 The Author(s). Published by Wolters Kluwer Health, Inc. DOI: 10.1097/MNM.0000000000001614

Pt radionuclides (radio-Pt) can directly trace the distribution of Pt-based drugs without changing their structures; in this regard, a radiotracer of Pt can provide precise pharmacokinetics data for Pt drugs. Radio-Pt with a suitable half-life enables highly quantitative evaluations until late time points irrespective of small injection doses or low accumulation of Pt in organs. ^{191}Pt ($T_{1/2}$ = 2.80 days, EC = 100%) is a good candidate radionuclide that has a suitable half-life and emits easily detectable γ/X-rays [13], enabling the highly quantitative and practical analysis of Pt drugs. Recently, we established a novel method for producing high-quality ^{191}Pt and radio-synthesized cisplatin (described as radio-cisplatin), as a model [14,15]. The radio-cisplatin product was obtained with a high radiochemical purity greater than 99%. Its lower detection limit at the femtomole scale (100 Bq of ^{191}Pt = 0.06 fmol), and it can work as a radiotracer for investigating pharmacokinetics. Here, a comprehensive and quantitative biodistribution assay with radio-cisplatin in mice bearing subcutaneous lung cancer was conducted.

Materials and methods

General

Chemicals and reagents were purchased from FUJIFILM Wako Pure Chemical (Osaka, Japan), Tokyo Chemical Industry (Tokyo, Japan), Kanto Chemical (Tokyo, Japan), Otsuka Pharmaceutical Factory (Tokyo, Japan), Tanaka Metal (Tokyo, Japan), Hayashi Pure Chemical Industry (Osaka, Japan), or Merck (Darmstadt, Germany). Milli-Q ultrapure water or diluted water was used for dilution in all experiments.

High-purity germanium (HPGe) γ-ray spectrometry was performed to measure the radioactivity of [^{189,191}Pt]cisplatin in saline before all in-vitro experiments. The HPGe detector (EGC 15–185-R; Eurisys Measures, Strasbourg, France) was coupled with a 4096 multichannel analyzer (RZMCA; Laboratory Equipment, Ibaraki, Japan) and calibrated using a mixed (^{109}Cd, ^{57}Co, ^{139}Ce, ^{51}Cr, ^{85}Sr, ^{137}Cs, ^{54}Mn, ^{88}Y, and ^{60}Co) standard source (Japan Radioisotope Association, Tokyo, Japan). A gamma counter (Wizard2 2-Detector Gamma Counter; PerkinElmer, Waltham, Massachusetts, USA) was used to measure radioactivity in biological samples. The X-rays and gamma-rays from both ^{191}Pt and ^{189}Pt were counted together under the energy window from 356 to 800 keV. Using an aliquot of the injection solution as a control for measurement, uptake was calculated from the radioactivity ratio of samples to the control.

Synthesis of [^{189,191}Pt]cisplatin

^{189,191}Pt was produced via the ^{nat}Ir(p, xn)^{189,191}Pt reaction in a 30 MeV proton beam for 2–3 h at a beam current of 10 μA at the NIRS-QST AVF-930 isochronous cyclotron, as described previously [14,15]. We used mixed ^{189,191}Pt, described as radio-Pt because ^{189}Pt ($T_{1/2}$ = 10.87 h, EC) is coproduced along with ^{191}Pt ($T_{1/2}$ = 2.83 days, EC) from a natural Ir target. [^{189,191}Pt]cisplatin (referred to as radio-cisplatin) was radio-synthesized from [^{189,191}Pt]$PtCl_4^{2-}$ and prepared in a saline solution [14]; the radiochemical purity at the end of synthesis (EOS) was 99+%. [^{189,191}Pt]cisplatin solution (500 kBq/ml, ^{189}Pt; 350 kBq/ml, ^{191}Pt at EOS) was used in all experiments.

Cell culture

The human lung cancer cell line NCI-H460 was obtained from ATCC (Manassas, Virginia, USA). The cells were cultured at 37 °C in a humidified atmosphere containing 5% CO_2 in RPMI-1640 (FUJIFILM Wako Pure Chemical) containing 10% fetal bovine serum (Thermo Fisher Scientific, Waltham, Massachusetts, USA).

Animal studies on the xenografted tumor model

The protocol for the animal experiments was approved by the Animal Care and Use Committee of the National Institutes for Quantum and Technology (13–1022, 26 May 2016), and all animal experiments were conducted following the institutional guidelines regarding animal care and handling. H460 cells were suspended in 1-ml PBS (2×10^7 cells/ml), and 2×10^6 cells in 100 μl were subcutaneously injected into the flank of male BALB/c-nu/nu mice (6 weeks old; CLEA Japan, Tokyo, Japan) under isoflurane anesthesia. Tumor volumes reached 100–400 mm^3 2–3 weeks after inoculation. For the biodistribution study, 100 μl of saline solution containing radio-cisplatin (50 kBq/^{189}Pt + 35 kBq/^{191}Pt) and 50 μg of nonradioactive cisplatin (2 mg/kg BW) were intravenously injected into mice when tumor volumes reached 100–400 mm^3 (n = 4 for each time-point). The mice were sacrificed by isoflurane inhalation at 2, 15, 60 min, 1, 3, 5, and 7 days after injection. Blood was obtained from the heart, and then tumor, lung, liver, pancreas, stomach, intestine, kidney, bone, and muscle were dissected. Uptake in tissues is represented as a percentage of the injected dose (%ID/g) (radioactivity) per gram of tissue and that for the whole body as a %ID. These values were corrected to those in the body weight of 20 g. Uptake in the whole body was calculated from the total radioactivity of dissected tissues and residual bodies.

Red blood cell partitioning and plasma protein binding of cisplatin

The red blood cell partitioning and the plasma protein binding of ^{191}Pt were evaluated for the blood of mice. At 2 min, 60 min, and 1 day after the intravenous injection of cisplatin, blood was obtained from the heart and mixed with heparin (Mochida Pharmaceutical Factory, Tokyo, Japan). The whole blood was centrifuged and divided into blood cells and plasma. The red blood cell partitioning rate of ^{191}Pt was calculated on the basis of the activity of blood and plasma, defined as $(A_{blood} - A_{plasma}) \times (1 - Hct) \times 100/A_{blood}) \times 100$, where A_{blood} is the radioactivity of 20 μl whole blood, A_{plama} is the radioactivity of a 20-μl plasma

fraction, and Hct is the hematocrit value (0.43). The plasma was ultrafiltered with Amicon Ultra (10 K, 0.5 ml Centrifugal Filters for DNA and Protein Purification and Concentration, Merck). The protein binding rate of ^{191}Pt was calculated based on the activity of each separated fraction, defined as $(A_{con} - A_{fil})/A_{con} \times 100$, where A_{con} is the radioactivity of a 50 µl concentrated fraction and A_{fil} is the radioactivity of a 50 µl filtered fraction.

Results

Using a radiotracer of cisplatin and exploiting its advantages, the quantitative pharmacokinetics of cisplatin for 7 days after the intravenous injection in subcutaneous tumor-bearing mice was evaluated. A previous study showed that radio-cisplatin uptake was dose-dependent and proportional to the administered concentration of cisplatin [15]. To provide data under dose conditions of chemotherapy in clinical settings, a mixed solution of radio-cisplatin and nonradioactive carriers (2 mg/kg BW) was injected. A lung cancer cell line, H460, was used in this study because cisplatin is commonly used as a chemotherapy agent for lung cancer [16,17].

First, the retention of cisplatin in the whole body and blood was investigated, as shown in Fig. 1, where data are shown as %ID for the whole body (Fig. 1, upper panel) and %ID per gram for blood (Fig. 1, lower panel). These results show a rapid clearance of cisplatin from the whole body and blood, consistent with the biphasic exponential curve including the alpha and beta phases (alpha, white; beta, black in Fig. 1). Cisplatin in the whole body was excreted quickly to ~24% of the injected dose within 19 h after injection, corresponding to the alpha phase of the retention curve (Fig. 1, upper panel, white). Thereafter, cisplatin was eliminated slowly during the beta phase, and ~10% of the injected dose remained in the body 7 days after injection (Fig. 1, upper panel, black). The blood concentration also decreased mainly within 19 h after injection, which corresponds to the alpha phase of the retention curve (Fig. 1, lower panel, white). Although the blood concentration was ~1%ID/g in the beta phase of the retention curve, the radiotracer enabled a quantitative evaluation (Fig. 1, lower panel, black).

Second, the biodistribution of cisplatin is shown in Fig. 2, where the data are represented as %ID/g of tissues. From the data in Fig. 2, the uptake ratio of each tissue to blood was summarized in Table 1 to evaluate the effect of blood on the accumulation in tissues. The uptake of cisplatin was high in the lungs and kidneys in the early time points after injection (Fig. 2). The accumulation in the lungs was related to blood clearance (Table 1). Renal accumulation of cisplatin was observed in the early time points, and its excretion was observed thereafter (Fig. 2). Hepatic accumulation was also observed, and the cisplatin uptake in the liver was relatively higher than that in the kidneys in the late time points (Fig. 2). There is a slight increase in the accumulation of cisplatin in the bone 5 days after injection (Fig. 2).

Third, the area under the curve ($AUC_{0\text{–}7\ days}$) was calculated on the basis of the biodistribution data (Fig. 1 lower panel and Fig. 2); the ratios of the tumor to each tissue are shown in Table 2. The accumulation in H460 tumors was not high; the peak was 4.7%ID/g 15 min after the injection (Fig. 2). Compared with the $AUC_{0\text{–}7\ days}$ in the pancreas, stomach, intestine, and muscle, that in H460 tumors was approximately the same or greater (Table 2). The $AUC_{0\text{–}7\ days}$ in the kidneys and liver were almost three times higher and that in the bone was almost two times higher than that in H460 tumors (Table 2).

As separate experiments, radio-cisplatin uptake in blood, the red blood cell partitioning rate of radio-cisplatin in blood cells, and the plasma protein binding rate of cisplatin were also evaluated at 2 min, 1 h, and 19 h after the injection (Table 3). The uptake in blood was ~35%ID/g at 2 min after injection and quickly decreased thereafter (Table 3), consistent with the results in Fig. 2. The red blood cell partitioning rate of cisplatin increased gradually over the experimental period after injection and reached ~50% (Table 3). The plasma protein binding rate of cisplatin increased to ~80% within 1 h after injection (Table 3). From the end of the alpha phase to the beginning of the beta phase, the plasma protein binding rates remained high (Table 3).

Discussion

This study evaluated the quantitative pharmacokinetics of cisplatin in mice bearing lung cancer for 7 days after intravenous injection with radio-cisplatin. The radio-Pt tracer showed the clearance of cisplatin from the whole body and blood, and the results were in good agreement with the pharmacological and pharmacokinetic properties of cisplatin. In addition, we investigated the comprehensive biodistribution of cisplatin to tissues with different degrees of drug accumulation over 7 days. Our results are consistent with the known clinical side effects of cisplatin and could provide reference data for the development of the next generation of Pt-based anticancer drugs. Because ^{191}Pt emits γ-rays and X-rays, which enable noninvasive imaging in humans, radio-Pt–based agents would provide comprehensive pharmacokinetics data not only in animals but also in humans.

The rapid clearance of cisplatin from the body and blood of mice intravenously injected with radio-cisplatin was observed. The blood concentration decreased immediately after injection and most of the injected cisplatin was excreted from the body by 1 day after injection. A biphasic retention curve in the whole body and blood was observed, and the biological half-life was calculated to be $T_{1/2}(\alpha) = 1.14$ h and $T_{1/2}(\beta) = 5.33$ days for the whole body and $T_{1/2}(\alpha) = 23.9$ min and $T_{1/2}(\beta) = 4.72$ days for blood (Fig. 1). This elimination of half-life in the blood is acceptably consistent with the results of previous studies [12,18,19].

Fig. 1

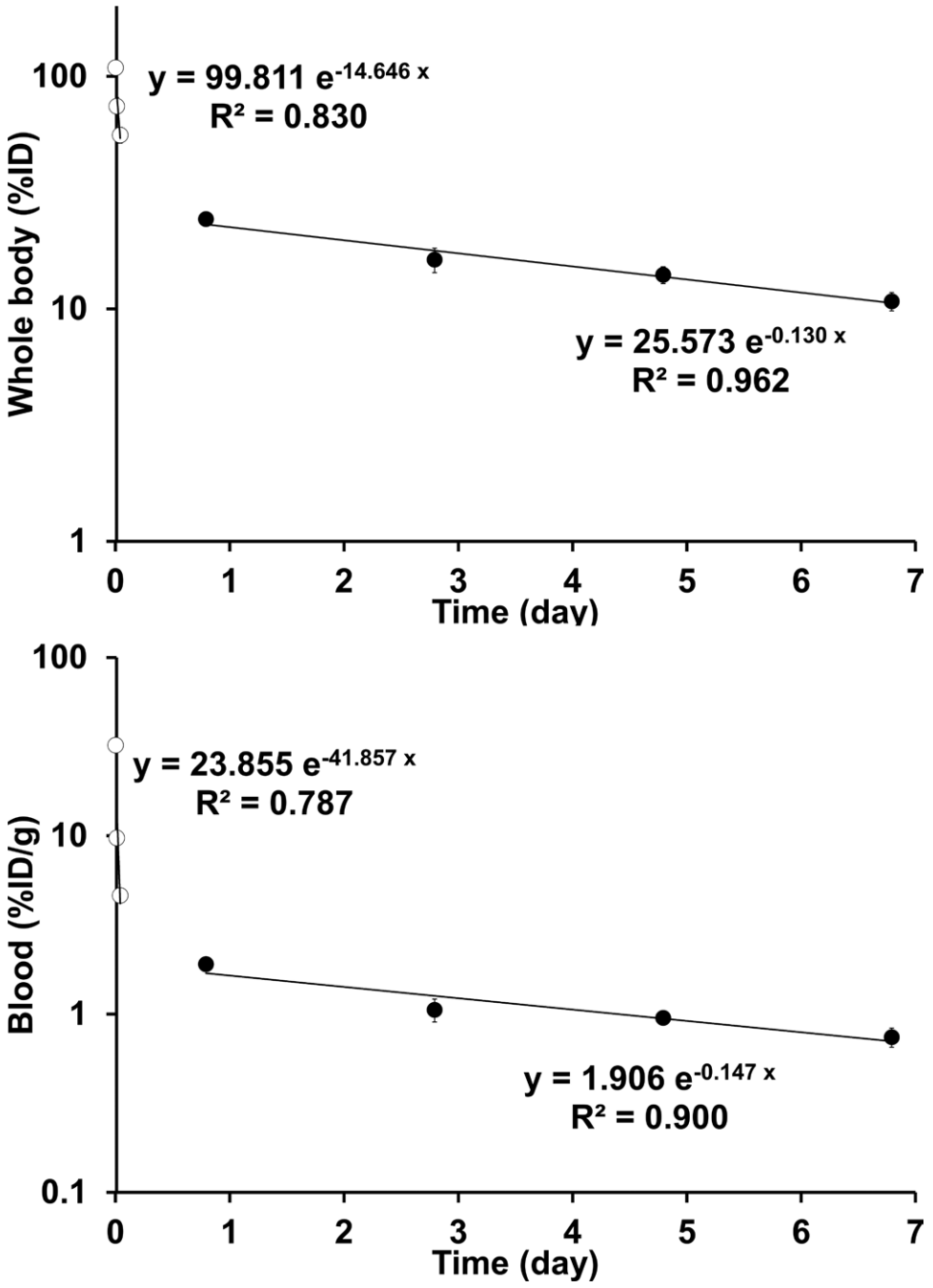

Percentage of the injected dose for the whole body (upper panel, %ID) and percentage of the injected dose per gram of blood (lower panel, %ID/g). Mice were intravenously injected with radio-cisplatin (50 kBq/^{189}Pt + 35 kBq/^{191}Pt) and with nonradioactive cisplatin (2 mg/kg body weight) in 100 µl of saline. Data are presented as the mean ± SD ($n = 4$). The alpha phase is indicated in white, and the beta phase is in black.

Our biodistribution experiments with radio-cisplatin over 7 days provided comprehensive pharmacokinetics data showing high accumulation in the kidneys, liver, and bone. The renal uptake increased in the early time points rapidly after injection, and radio-cisplatin was excreted gradually in the late time points (Fig. 2). According to the literature, cisplatin is rapidly excreted via the kidneys although a part of it remains intact [12,19]. Most of the intact cisplatin would be excreted via the kidneys rapidly after injection before working in the body. Some intact cisplatin was uptaken into renal cells, inducing renal disorder as the main side effect of cisplatin [7]. This uptake into renal cells and their disorder could be caused by a rapid distribution of intact cisplatin in the early time points; this interpretation is supported

Fig. 2

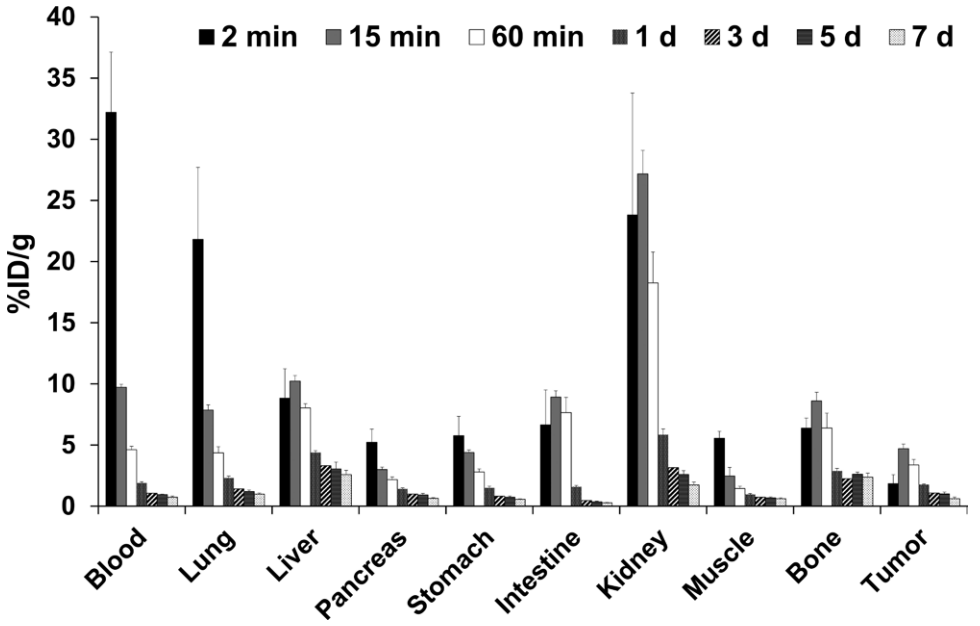

Biodistribution of radio-cisplatin in mice bearing H460 tumors. Data are represented as the percentage of the injected dose per gram (%ID/g) of tissues (mean ± SD, $n = 4$). The data for blood are the same as in the lower panel of Fig. 1.

Table 1 Uptake ratios of each tissue to blood

Tissue/ blood	2 min	15 min	60 min	1 day	3 days	5 days	7 days
Lung	0.68	0.81	0.94	1.21	1.34	1.26	1.34
Liver	0.27	1.05	1.74	2.30	3.13	3.20	3.48
Pancreas	0.16	0.31	0.47	0.75	0.94	0.98	0.87
Stomach	0.18	0.45	0.61	0.79	0.77	0.77	0.76
Intestine	0.21	0.92	1.65	0.83	0.44	0.39	0.38
Kidney	0.74	2.79	3.95	3.07	2.98	2.72	2.35
Muscle	0.17	0.25	0.31	0.50	0.70	0.72	0.82
Bone	0.20	0.89	1.38	1.51	2.13	2.74	3.20
Tumor	0.06	0.48	0.73	0.93	1.02	1.07	0.83

The ratios were calculated on the basis of the biodistribution data in Fig. 2.

Table 2 Area under the curve ($AUC_{0-7\ days}$) ratios of tumor to each tissue

Tumor/tissue	$AUC_{0-7\ days}$ ratio
Blood	0.91
Lung	0.76
Liver	0.35
Pancreas	1.17
Stomach	1.24
Intestine	1.18
Kidney	0.30
Muscle	1.59
Bone	0.46

The ratios were calculated on the basis of the biodistribution data in Fig. 2. AUC, area under the curve.

by our radio-cisplatin results. Uptake in the liver was relatively higher than in the kidneys in the late time points from 3 days after injection. This result might be related to the plasma protein binding of cisplatin. The plasma protein binding rate increased immediately after intravenous injection (Table 3), which is consistent with our understanding of the behavior of cisplatin [9–12,18,19]. Cisplatin easily reacts with sulfur-containing cysteine or methionine of proteins such as serum albumin [20–22], leading to an irreversible increase of protein-bound cisplatin. The protein-bound cisplatin is known to not be excreted predominately by the kidneys, to be retained longer in the blood, and to be accumulated in the liver [23,24]. This tendency might be responsible for the moderate retention in the liver in the late time points (Fig. 2), suggesting that the protein-bound cisplatin would be reaccumulated partly in the liver while remaining and circulating in the blood (Fig. 2). Numerous previous studies on cisplatin treatments have shown that high-dose administration of cisplatin causes hepatoxicity [25–27], and the oxidative stress derived from the metal toxicity of Pt has been suggested to be the main cause [28–30]. Some authors have also reported a high accumulation of cisplatin in the liver [31–34]. The radio-Pt tracer could provide insights enabling the elucidation of the relationship between hepatoxicity and cisplatin. Only the bone uptake of cisplatin increased slightly on day 5. Cisplatin remaining in blood or excreted from tissues appeared to be taken into bones. This effect is speculated to correspond to cisplatin side effects such as myelosuppression. Collectively, our comprehensive and quantitative biodistribution results provide insights into the cause of the adverse effects of cisplatin.

As a limitation of this study, the clearance rate was the result of a single and rapid administration of cisplatin in

Table 3 Uptake in whole blood (%ID/g), red blood cell partitioning rate (%), and plasma protein binding rate (%) ($n = 2$)

Time	Whole blood uptake (%ID/g)	Red blood cell partitioning rate (%)	Plasma protein binding rate (%)
2 min	33.7, 35.5	1.5, 8.8	35.5, 28.6
1 h	4.5, 5.0	27.3, 23.2	82.8, 79.5
19 h	1.9, 2.2	51.8, 55.7	91.6, 92.2

%ID, percentage of the injected dose.

mice (2 mg/kg body weight). According to previous studies [35–41], the administration protocol affects the clearance and the therapeutic efficacy of cisplatin. Numerous protocols are used in clinical settings, and maintaining a constant blood drug concentration at the optimal administration rate is important [35–41]. The radiotracer can enable such systematic investigations of the effect of the administration rate of cisplatin. Although our results are consistently discussed in relation to the clinical properties of cisplatin, further preclinical studies should be conducted for target regimens. In addition, our results are based on directly quantifying radio-Pt, which is a basic factor of the cytotoxic action of cisplatin. The biodistribution included both intact and protein-bound cisplatin, and metabolite analyses were not conducted.

Conclusion

This study clearly showed that a radio-Pt tracer is useful for acquiring comprehensive and quantitative biodistribution data because it can be detected quantitatively with high sensitivity. This work supports the current understanding of the pharmacological and pharmacokinetic properties of cisplatin and provides reference data for the further development of Pt-based drugs.

Acknowledgements

The authors would like to thank the cyclotron staff for operating the NIRS cyclotron AVF-930. We are grateful to Hisashi Suzuki, Akihito Abe, and Ayumi Kadoma for technical support.

This work was supported in part by JSPS KAKENHI Grant Number JP20J20518.

Conflicts of interest

There are no conflicts of interest.

References

1 Johnstone TC, Suntharalingam K, Lippard SJ. The next generation of platinum drugs: targeted Pt(II) agents, nanoparticle delivery, and Pt(IV) prodrugs. *Chem Rev* 2016; **116**:3436–3486.
2 Alderden RA, Hall MD, Hambley TW. The discovery and development of cisplatin. *J Chem Educ* 2006; **83**:728.
3 Wang D, Lippard SJ. Cellular processing of platinum anticancer drugs. *Nat Rev Drug Discov* 2005; **4**:307–320.
4 Jamieson ER, Lippard SJ. Structure, recognition, and processing of cisplatin-DNA adducts. *Chem Rev* 1999; **99**:2467–2498.
5 Gately DP, Howell SB. Cellular accumulation of the anticancer agent cisplatin: a review. *Br J Cancer* 1993; **67**:1171–1176.
6 Eljack ND, Ma HY, Drucker J, Shen C, Hambley TW, New EJ, *et al*. Mechanisms of cell uptake and toxicity of the anticancer drug cisplatin. *Metallomics* 2014; **6**:2126–2133.
7 Crona DJ, Faso A, Nishijima TF, McGraw KA, Galsky MD, Milowsky MI. A systematic review of strategies to prevent cisplatin-induced nephrotoxicity. *Oncologist* 2017; **22**:609–619.
8 Hermann G, Heffeter P, Falta T, Berger W, Hann S, Koellensperger G. *In vitro* studies on cisplatin focusing on kinetic aspects of intracellular chemistry by LC-ICP-MS. *Metallomics* 2013; **5**:636–647.
9 Falta T, Koellensperger G, Standler A, Buchberger W, Maderc RM, Hann S. Quantification of cisplatin, carboplatin and oxaliplatin in spiked human plasma samples by ICP-SFMS and hydrophilic interaction liquid chromatography (HILIC) combined with ICP-MS detection. *J Anal At Spectrom* 2009; **24**:1336–1342.
10 Hennik MB, Vijgh WJF, Klein I, Elferink F, Vermorken JB, Winograd B, *et al*. Comparative pharmacokinetics of cisplatin and three analogues in mice and humans. *Cancer Res* 1987; **47**:6297–6301.
11 Urien S, Lokiec F. Population pharmacokinetics of total and unbound plasma cisplatin in adult patients. *Br J Clin Pharmacol* 2004; **57**:756–763.
12 DeConti RC, Toftness BR, Lange RC, Creasey WA. Clinical and pharmacological studies with cis-diamminedichloroplatinum (II). *Cancer Res* 1973; **33**:1310–1315.
13 NuDat 3.0: a software product developed by National Nuclear Data Center (NNDC) at Brookhaven National Laboratory, http://www.nndc.bnl.gov/nudat2/index.jsp.
14 Obata H, Minegishi K, Nagatsu K, Ogawa M, Zhang MR. Synthesis of no-carrier-added [188, 189, 191Pt]cisplatin from a cyclotron produced 188, 189, 191PtCl42- complex. *Sci Rep* 2021; **11**:8140.
15 Obata H, Tsuji AB, Sudo H, Sugyo A, Minegishi K, Nagatsu K, *et al*. *In Vitro* evaluation of no-carrier-added radiolabeled cisplatin ([189, 191Pt]cisplatin) emitting auger electrons. *Int J Mol Sci* 2021; **22**:4622.
16 Schiller JH, Harrington D, Belani CP, Langer C, Sandler A, Krook J, *et al*; Eastern Cooperative Oncology Group. Comparison of four chemotherapy regimens for advanced non-small-cell lung cancer. *N Engl J Med* 2002; **346**:92–98.
17 Temel JS, Greer JA, Muzikansky A, Gallagher ER, Admane S, Jackson VA, *et al*. Early palliative care for patients with metastatic non-small-cell lung cancer. *N Engl J Med* 2010; **363**:733–742.
18 Panteix G, Beaujard A, Garbit F, Chaduiron-Faye C, Guillaumont M, Gilly F, *et al*. Population pharmacokinetics of cisplatin in patients with advanced ovarian cancer during intraperitoneal hyperthermia chemotherapy. *Anticancer Res* 2002; **22**:1329–1336.
19 Vermorken JB, van der Vijgh WJ, Klein I, Gall HE, van Groeningen CJ, Hart GA, Pinedo HM. Pharmacokinetics of free and total platinum species after rapid and prolonged infusions of cisplatin. *Clin Pharmacol Ther* 1986; **39**:136–144.
20 Wang And X, Guo Z. The role of sulfur in platinum anticancer chemotherapy. *Anticancer Agents Med Chem* 2007; **7**:19–34.
21 Ivanov AI, Christodoulou J, Parkinson JA, Barnham KJ, Tucker A, Woodrow J, Sadler PJ. Cisplatin binding sites on human albumin. *J Biol Chem* 1998; **273**:14721–14730.
22 Zimmermann T, Zeizinger M, Burda JV. Cisplatin interaction with cysteine and methionine, a theoretical DFT study. *J Inorg Biochem* 2005; **99**:2184–2196.
23 Wolf WC. Preparation and metabolism of a cisplatin/serum protein complex. *Chem Biol Interact* 1980; **30**:223–235.
24 Holding JD, Lindup WE, van Laer C, Vreeburg GC, Schilling V, Wilson JA, Stell PM. Phase I trial of a cisplatin-albumin complex for the treatment of cancer of the head and neck. *Br J Clin Pharmacol* 1992; **33**:75–81.
25 Cersosimo RJ. Hepatotoxicity associated with cisplatin chemotherapy. *Ann Pharmacother* 1993; **27**:438–441.
26 Rashid NA, Halim SASA, Teoh SL, Budin SB, Hussan F, Ridzuan NRA, *et al*. The role of natural antioxidants in cisplatin-induced hepatotoxicity. *Biomed Pharmacother* 2021; **144**:112328.
27 Lu Y, Cederbaum AI. Cisplatin-induced hepatotoxicity is enhanced by elevated expression of cytochrome P450 2E1. *Toxicol Sci* 2006; **89**:515–523.
28 Liu J, Liu Y, Habeebu SS, Klaassen CD. Metallothionein (MT)-null mice are sensitive to cisplatin-induced hepatotoxicity. *Toxicol Appl Pharmacol* 1998; **149**:24–31.
29 Naziroglu M, Karaoğlu A, Aksoy AO. Selenium and high dose vitamin E administration protects cisplatin-induced oxidative damage to renal, liver and lens tissues in rats. *Toxicology* 2004; **195**:221–230.
30 Christova TY, Gorneva GA, Taxirov SI, Duridanova DB, Setchenska MS. Effect of cisplatin and cobalt chloride on antioxidant enzymes in the livers

of Lewis lung carcinoma-bearing mice: protective role of heme oxygenase. *Toxicol Lett* 2003; **138**:235–242.
31 Lange RC, Spencer RP, Harder HC. The antitumor agent cis-Pt(NH 3) 2 Cl 2: distribution studies and dose calculations for 193m Pt and 195m Pt. *J Nucl Med* 1973; **14**:191–195.
32 Lange RC, Spencer RP, Harder HC. Synthesis and distribution of a radiolabeled antitumor agent: cis-diamminedichloroplatinum. II. *J Nucl Med* 1972; **13**:328–330.
33 Areberg J, Björkman S, Einarsson L, Frankenberg B, Lundqvist H, Mattsson S, *et al*. Gamma camera imaging of platinum in tumours and tissues of patients after administration of 191Pt-cisplatin. *Acta Oncol* 1999; **38**:221–228.
34 Smith HS, Taylor DM. Distribution and retention of the antitumor agent 195mPt-cis-dichlorodiammine platinum (II) in man. *J Nucl Med* 1974; **15**:349–351.
35 Jordan NS, Schauer PK, Schauer A, Nightingale C, Golub G, Martin RS, Williams HM. The effect of administration rate on cisplatin-induced emesis. *J Clin Oncol* 1985; **3**:559–561.
36 Ludwig R, Alberts DS, Miller TP, Salmon SE. Evaluation of anticancer drug schedule dependency using an *in vitro* human tumor clonogenic assay. *Cancer Chemother Pharmacol* 1984; **12**:135–141.
37 Drewinko B, Brown BW, Gottlieb JA. The effect of cis-diamminedichloroplatinum (II) on cultured human lymphoma cells and its therapeutic implications. *Cancer Res* 1973; **33**:3091–3095.
38 Matsushima Y, Kanzawa F, Hoshi A, Shimizu E, Nomori H, Sasaki Y, Saijo N. Time-schedule dependency of the inhibiting activity of various anticancer drugs in the clonogenic assay. *Cancer Chemother Pharmacol* 1985; **14**:104–107.
39 Salem P, Khalyl M, Jabboury K, Hashimi L. Cis-diamminedichloroplatinum (II) by 5-day continuous infusion. A new dose schedule with minimal toxicity. *Cancer* 1984; **53**:837–840.
40 Posner MR, Ferrari L, Belliveau JF, Cummings FJ, Wiemann MC, O'Rourke A, *et al*. A phase I trial of continuous infusion cisplatin. *Cancer* 1987; **59**:15–18.
41 Creagan ET, Richardson RL, Kovach JS. Pilot study of a continuous five-day intravenous infusion of etoposide concomitant with cisplatin in selected patients with advanced cancer. *J Clin Oncol* 1988; **6**:1197–1201.